STRUCTURE OF TAYLOR VORTEX FLOW AND THE INFLUENCE OF SPATIAL AMPLITUDE VARIATIONS ON PHASE DYNAMICS

D. Roth[1], M. Lücke[1], M. Kamps[2], and R. Schmitz[3]

[1]*Institut für Theoretische Physik, Universität des Saarlandes D–6600 Saarbrücken, FRG*
[2]*Höchstleistungsrechenzentrum, Stabsstelle Supercomputing D–5170 Jülich, FRG*
[3]*Forschungszentrum Jülich GmbH, Institut für Festkörperforschung D–5170 Jülich, FRG*

In the first part the spatial structure of Taylor vortices at moderate supercritical Reynolds numbers is analysed in detail using 2–dimensional numerical simulation data. For radius ratios $\eta = 0.75, 0.88$ the dependence of axial Fourier modes on the Reynolds number is presented in the case where only the inner cylinder rotates as well as for co — and counterrotating outer cylinder. In the second part the dynamical response of the vortex structure to small perturbations is investigated, in particular for the experimentally relevant situations where the amplitude of the flow is not constant over the whole systems. A simple generalized diffusion equation for the phase is derived. The space dependence of the amplitude R(z) influences the time evolution of the phase of the structure. In the experimentally most common case of a finite system with rigid end plates the amplitude enhancement near the ends (Ekman vortex) leads to a substantial increase of the long–time relaxation rate of the phase. Quantitative agreement between phase description and numerical simulation of the full Navier Stokes equations is found and qualitative agreement with experimental results.

The Taylor–Couette system shows a rich variety of interesting features and allows quantitative experimental as well as theoretical studies. Extensions of G.I. Taylor's fundamental work[1] as changes in the geometry, different fluids, additional forces (heat, rotation, pressure, modulation) have discovered new patterns and bifurcation scenarios. But there are also tasks left in the original setup. Two of them we want to attack in this paper: First we will study the nonlinear structure of the Taylor vortices in detail which has not yet been done for independently driven outer and inner cylinders. Secondly we will investigate the influence of end plates involving Ekman vortices on the phase diffusion response of the Taylor rolls.

NOTATION AND INVESTIGATION METHOD

Two co–axial cylinders of length L, radii R_1 and R_2, gapwidth $d = R_2 - R_1$, rotating with angular velocities Ω_1 and Ω_2 are considered. The system properties are

Ordered and Turbulent Patterns in Taylor-Couette Flow
Edited by C.D. Andereck and F. Hayot, Plenum Press, New York, 1992

given by a radius ratio $\eta = R_1/R_2$, a rotation ratio $\mu = \Omega_2/\Omega_1$, and a control parameter $\epsilon = \Omega_1/\Omega_{1c} - 1$ relative to the critical velocity Ω_{1c} for the onset of Taylor vortices at $\mu = 0$. The fluid velocity is decomposed in cylindrical coordinates $\mathbf{u} = ue_r + ve_\varphi + we_z$.

The full axisymmetric Navier–Stokes equations are solved numerically using a SOLA version of the MAC finite difference scheme with an iterative solver for the pressure[2]. Boundary conditions at top and bottom ends are periodic for the structure investigation and rigid in the phase diffusion case.

STRUCTURE OF STATIONARY TAYLOR VORTICES

Since there is no closed expression describing the shape of Taylor rolls in the η, μ, ϵ–parameter space, one needs a lot of single data to cover the whole range of interest. Most authors[3,4] in the literature have restricted their analyses to μ=0, the case when only the inner cylinder is rotating. Recently $\mu \neq 0$, in particular $\mu < 0$, the counterrotating case, has been attracting much interest. Hence we present here the μ–dependence of some characteristic values, as the axial Fourier coefficients of the fields and the radial position of the roll centers. Those data can be useful to determine

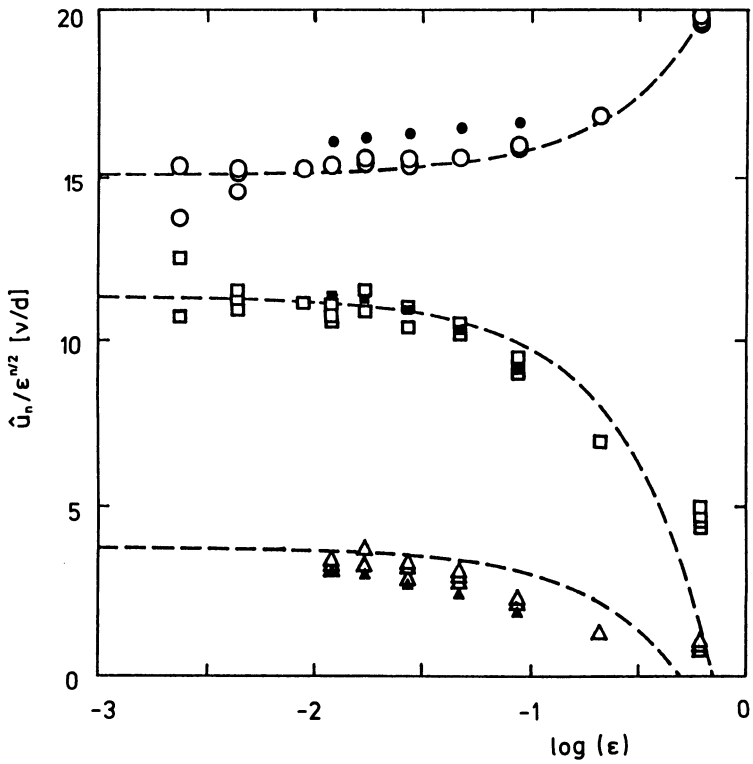

Fig. 1. Fourier coefficients of the radial velocity in the middle of the gap vs the control parameter ϵ. Open (full) symbols refer to radius ratio $\eta = 0.75$ (0.893), circles belong to n = 1, squares to n = 2, and triangles to n = 3. Dashed lines are fits to the $\eta = 0.75$–data according to eq. (1).

the validity range of model representations of the Taylor vortices like the Ginzburg–Landau equation (GLE) or few–mode Galerkin models, and to compare the change of structure caused by external forces as pointed out in the introduction.

According to Davey[5] we decompose the radial velocity

$$u(r,z) = \sum_{n=1}^{\infty} \hat{u}_n(r) \cos(nkz) \tag{1a}$$

where the Fourier coefficients $\hat{u}_n(r)$ have the form

$$\hat{u}_n(r) = \epsilon^{n/2} A_n(r) [1 + \epsilon B_n(r)]. \tag{1b}$$

Similar expressions hold for v, w and the pressure p. Fig. 1 recalls[4] the way how we get the amplitudes A_n and B_n. For $\eta = 0.75$ and $\eta = 0.88$ the Fourier coefficients are plotted versus ϵ. The different values belong to various k. Davey's formula (1) holds quite well and the results depend weakly on η. The A_n and B_n found by fitting the numerically obtained data to eq. (1b) are compiled in table 1. The quotient A_2/A_1 is rather large which turns out to be the typical situation for counterrotating cylinders (see below). Consequently an accurate description of Taylor vortex flow requires more than only one Fourier mode. That is also obvious from the inflow/outflow asymmetry. A second remark on table 1 is that the correction terms B_n are large in comparison to 1 except for the case of w_1. Due to this fact the w–component is the best choice for a single–mode representation of Taylor rolls.

Fig. 2 shows the μ–dependence of the Fourier coefficients. Since the radial shape changes with μ we have taken the position where $|\hat{u}_n(r)|$ is maximal. These maximum

Table 1. Coefficients obtained by fitting the first three Fourier coefficients $\hat{u}_n$, $\hat{w}_n$, $\hat{p}_n$, for small ϵ by $\epsilon^{n/2}$ $A_n(1 + \epsilon B_n)$. Units are d for r, ν/d for the velocities, and $\rho\, \nu^2/d^2$ for p.

	$u(r_1 + \frac{1}{2})$	$w(r_1 + \frac{1}{4})$	$p(r_1 + \frac{1}{4})$
A_1	15.2	15.8	− 214
B_1	0.5	− 0.07	− 0.34
A_2	11.1	− 6.0	26
B_2	− 1.4	2.3	4.3
A_3	3.5	1.4	− 44
B_3	− 2.0	− 0.25	− 1.3

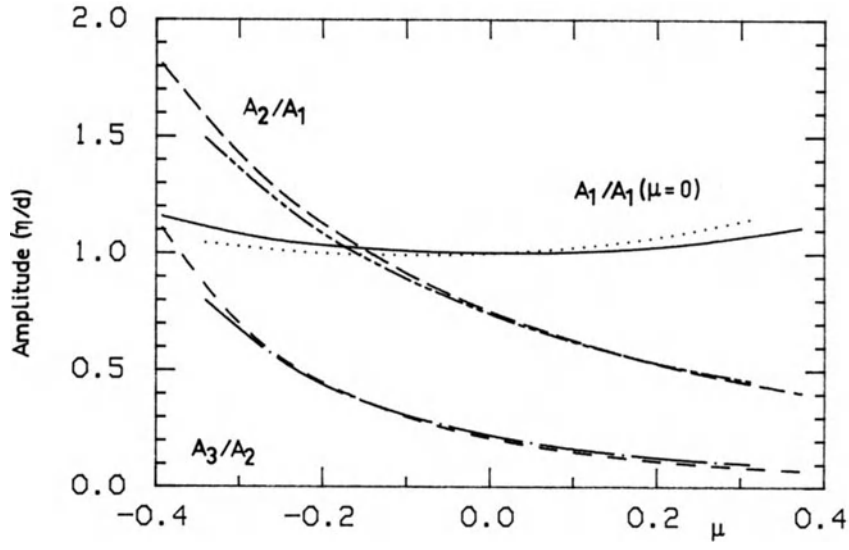

Fig. 2. μ–variation of the Fourier coefficients of u in the small ϵ limit, i. e. $\hat{u}_n \simeq \epsilon^{n/2} A_n$. For the first coefficient $A_1(\mu)/A_1(\mu = 0)$ is taken, the higher ones (n = 2,3) are divided by $A_1(\mu)$. The radial position is where u(r) is extremal. Lines types are (i) $\eta = 0.75$ n=1: full line, n=2: long dashed, n=3: short dashed and (ii) $\eta = 0.88$ n=1: dotted, n=2:dash–dot–dotted, n=3: dash–dotted.

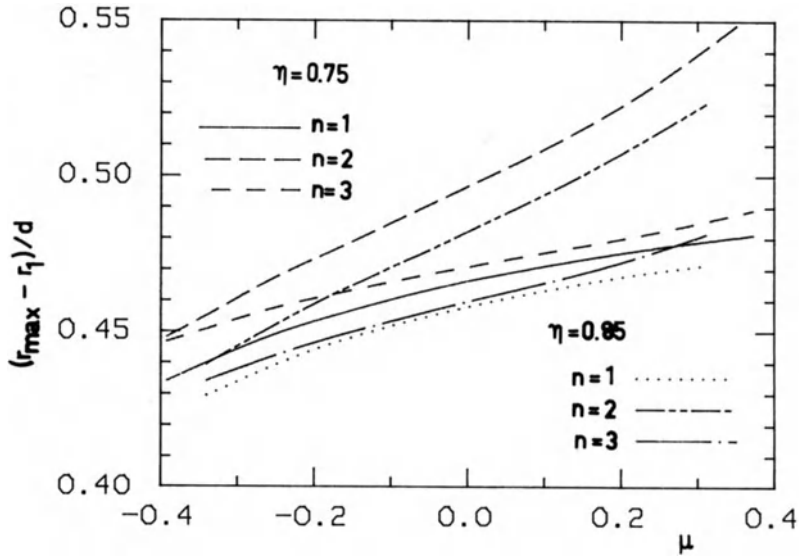

Fig. 3. Radial locations of the maximum of $A_n(r)$ (see Fig. 2) as a function of μ. Line types as in Fig. 2.

locations are drawn in Fig. 3. Lowering η shift them inwards, while the coefficients themselves hardly change. However, there are small differences in the scaling: $A_1(\eta = 0.88,\ \mu = 0) = 16.5$, while $A_1(\eta = 0.75,\ \mu = 0) = 15.7$ (see Fig. 1). The first coefficient is almost μ–independent, while the higher ones increase with lowering μ. Thus the contribution by higher axial Fourier modes to Taylor vortex flow increases strongly when lowering μ from the $\mu = 1$ limiting case. This in turn restricts the application range of the lowest–order GLE as a quantitative method to describe Taylor vortices already at $\mu = 0$ and even more so at negative μ. In contrast to that Rayleigh–Bénard convection – corresponding for a Prandtl number of 1 to the $\eta \to 1$, $\mu \to 1$ limit of the Taylor system – is much better represented by just one Fourier mode.

PHASE DYNAMICS

To explain what we are dealing with when speaking about phase dynamics we shortly describe an experiment done by Gerdts[6]. He used a Taylor system ($\eta = 0.5$, $\mu = 0$) with a movable top plate. First, stationary Taylor rolls were prepared. Then the top plate was moved downwards a little. This causes the vortices to adjust to their new positions basically without changing their strength. By looking at a particular vortex one can see the center position relax into its final location with an exponential long–time behavior. This suggests[7] a treatment with a diffusion equation for a phase variable connected to the vortex location

$$\partial_t \psi = D_0 \partial_x^2 \psi. \tag{2}$$

Here $D_0 = \xi_0^2/\tau_0 \simeq 1.92$ is the diffusion constant for an infinitely long system. In Fig. 4 the experimental long–time relaxation rates[6] divided by those expected from eq. (2) are plotted for different lengths and control parameter values (open symbols). They all lie well above unity tending to increase with decreasing ϵ. Here we want to show that this peculiar increase is related to the Ekman enhancement of the Taylor vortex flow amplitude near the end which is not properly accounted for by eq. (2).

To do so we start with the usual GLE for the amplitude A of a velocity component[8],

$$u(r,z,t) = A(z,t)e^{ik_c z}\hat{u}(r) + c.c. \tag{3a}$$

which reads

$$\tau_0 \partial_t A(z,t) = \left[\xi_0^2 \partial_z^2 + \epsilon - g|A(z,t)|^2\right] A(z,t). \tag{3b}$$

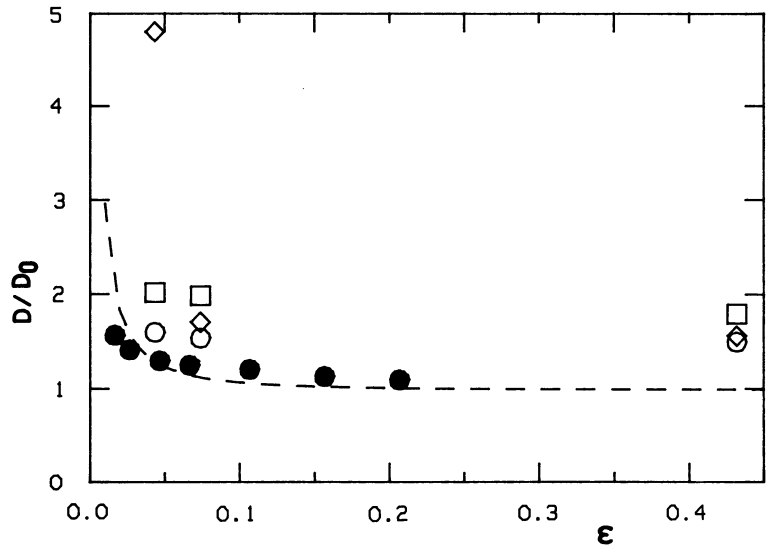

Fig. 4. ϵ—dependence of the effective diffusion constant D divided by the infinite—system value D_0. The dashed line is the result of formula (6). Filled circles come from the numerical solution of the full NSE with L = 25, $\eta = 0.75$. Open circles (diamonds, squares) are the $\eta = 0.5$ experimental findings of Gerdts[6] for L = 20.3 (12.4, 8.3).

A decomposition of $A = Re^{i\phi}$ into phase ϕ and modulus R yields the generalized diffusion equation

$$R^2(z)\,\partial_t\varphi\,(z,t) = D_0 R^2(z)\,\partial_z^2\varphi\,(z,t) + D_0[\partial_z R^2(z)]\partial_z\varphi(z,t) \qquad (4)$$

for the deviation $\varphi(z,t) = \phi(z,t) - \phi(z,t = \infty)$ from the final stationary phase. In eq. (4) we have assumed that the timescale of the amplitude relaxation is short compared to the relaxation time $L^2/(\pi^2 D_0)$ of the phase. Thus we drop the time dependence of R and consider it to be already stationary during the long–time relaxation of φ to zero. R(z) can be taken as input, for instance from the envelope of the measured velocity profile. Eq. (4) reduces to eq. (2) if R(z) is constant. Thus we want to emphasize that a nonuniform envelope of the velocity profile R(z) changes the time evolution of the phase of the vortex chain.

After inserting $\varphi(z,t) = \sum_n \varphi_n(t)\sqrt{2}\sin(n\pi z/L)$ eq. (4) reduces to an algebraic eigenvalue problem[4]. The smallest eigenvalue gives the long–time behaviour of φ. The very first approximation of this eigenvalue can be obtained by truncating the infinite dimensional system of equations to a 1x1–system. Then we get the effective diffusion constant D with

$$\frac{D}{D_0} \simeq \frac{R_0 + 3R_2}{R_0 - R_2} \quad ; \quad R_j = \frac{1}{L}\int_0^L dz\, R(z) \cos\frac{j\pi z}{L}. \tag{5}$$

Within this drastic truncation D depends on the size of the second axial Fourier–cosine projection of R(z), R_2. Thus $D > D_0$ if R_2 is positive.

We now turn to investigate the influence of Ekman vortices in a finite system. As sketched out in Fig. 5, the rigid boundary condition on both ends causes Ekman vortices leading to an enhancement of the modulus R(z) near the ends. Here $R_2 > 0$, so we expect $D > D_0$. In order to see analytically the influence of the length L and the control parameter ϵ on the effective diffusion constant we model R(z) for convenience with two exponentials

$$R(z) \simeq A_0 + B\left[\exp(\frac{-z}{\ell}) + \exp(\frac{L-z}{\ell})\right] \tag{6a}$$

rather than the correct Jacobian double periodic function. We take the ϵ–dependence of the bulk amplitude A_0 and of the penetration length ℓ of the Ekman vortex from the GLE (3), while the strength B of the Ekman vortex is fitted empirically. Then we get

$$A_0 = \sqrt{\epsilon/g} \quad ; \quad \ell \simeq \xi_0/\sqrt{\epsilon} \tag{6b}$$

$$A_0 + B \simeq B_0 + \epsilon B_1 \quad ; \quad B_0, B_1 \text{ constant.} \tag{6c}$$

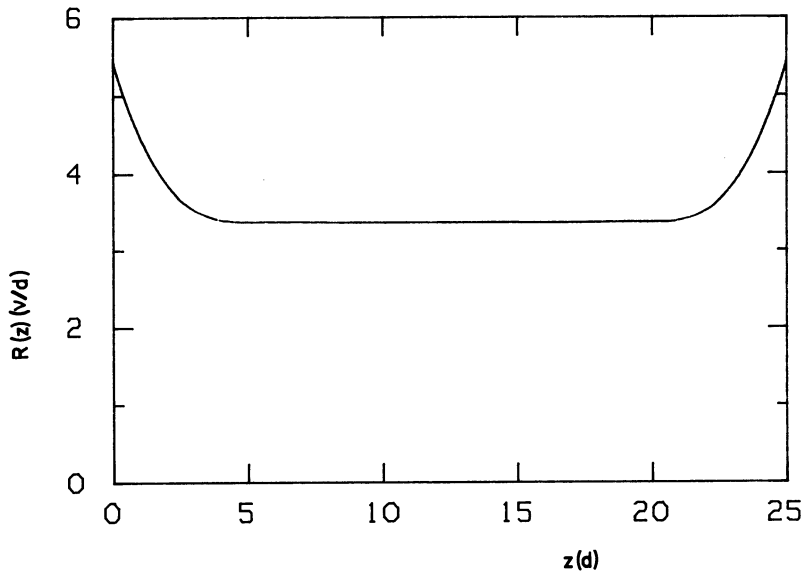

Fig. 5. Modulus R(z) of the amplitude of the radial velocity field in a system with two rigid ends, L = 25, ϵ = 0.047, η = 0.75.

Inserting the representation (6) into the approximation (5) gives an expression for D/D_0 in the presence of rigid end plates

$$\frac{D}{D_0} \simeq 1 + \frac{8B\ell}{A_0 L} = 1 + \frac{8\xi_0 g^{1/2}}{L}(B_0\epsilon^{-1} - g^{-1/2}\epsilon^{-1/2} + B_1). \tag{7}$$

The correction to 1 shows an offset for larger ϵ due to B_1. Within the 1x1 matrix truncation D diverges for $\epsilon \to 0$. With increasing truncation order of the eigenvalue problem, however, there is a rounding off. To check our simple model results (5–7) we performed a numerical simulation ($L = 25$, $\eta = 0.75$, $\mu = 0$) of the *full* NSE with the correct boundary conditions[4]. These results are shown in Fig. 4. The numerical data (filled circles) agree surprisingly well with our simple model formula (7). Note in particular the substantial increase of D/D_0 to about 1.6 near $\epsilon = 0$. The experimental points of Gerdts do not fit quantitatively, but in their general tendency. One must keep in mind that it is more difficult to control the boundary conditions in experiments than in numerical simulations. Further experimental work should be done to test our predictions.

REFERENCES

1 G. I. Taylor, Phil. Trans R. Soc. Lond. A **223,** 289 (1923).

2 C. W. Hirt, B. D. Nichols, and N. C. Romero, Los Alamos Scientific Laboratory Report LA–5852, 1975. See also M. Lücke, M. Mihelcic, and K. Wingerath, Phys. Rev. A **31,** 396 (1985).

3 H. A. Snyder and R. B. Lambert, J. Fluid Mech. **26,** 545 (1966); J. P. Gollub and M. H. Freilich, Phys. Fluids **19,** 295 (1977); H. Fasel and O. Booz, J. Fluid Mech. **138,** 21 (1984); T. Berland, T. Jǿssang, and J. Feder, Phys. Scr. **34,** 427 (1986); R. M. Heinrichs, D. S. Cannell, G. Ahlers, and M. Jefferson, Phys. Fluids **31,** 250 (1988); H. Kuhlmann, D. Roth, and M. Lücke, Phys. Rev. A **39,** 745 (1989).

4 M. Lücke and D. Roth, Z. Phys. B **78,** 147 (1990).

5 A. Davey, J. Fluid Mech. **14,** 336 (1962).

6 U. Gerdts, Ph. D. Thesis, Kiel 1985 (unpublished).

7 P. Tabeling, J. Phys. (Paris) Lett. **44,** L665 (1983); for a review concerning phase dynamics see: H. Brand, in: *Pattern, Defects, and Materal Instabilities,* D. Walgraef and N. M. Ghoniem (ed.), NATO ASI Series E, vol. **183,** Kluwer, Dordrecht, (1990), p. 25.

8 R. Graham and J. A. Domeradzki, Phys. Rev. A **26,** 1572 (1982).